Zeitschrift: IABSE reports = Rapports AIPC = IVBH Berichte
Band: 79 (1998)

Rubrik: Plenary session: Long-span bridges. Keynote lectures

Plenary Session

Long-Span Bridges

Keynote Lectures

Leere Seite
Blank page
Page vide

Long Span Cable Supported Bridges: Present Technology and Trends

Niels J GIMSING
Professor
Techn. Univ. of Denmark
Lyngby, Denmark

Niels J Gimsing, born 1935, is professor at the Technical University of Denmark since 1976. From 1970 he has acted as a bridge design adviser during feasibility studies and in the design phase for the Storebaelt Bridge. Since 1993 he has been a member of the design team in the ASO Group during design of the Oeresund Bridge.

Summary

The activity within the field of long span cable supported bridges has never been larger than at the end of the 20th century. The technology is well advanced to cope with the present challenges but it is also approaching its limits so if the trend towards ever increasing span lengths continues into the next century, further developments are required to ensure that the bridges will be stable, durable and constructible.

1. Introduction

During the 1990s the construction of long-span cable supported bridges has experienced a considerable development. This is illustrated in Table 1 and 2 listing the ten longest cable-stayed bridges and suspension bridges, respectively. It appears that all of the listed cable-stayed bridges will have been completed during the 1990s, and in the same decennium also five of the ten longest suspension bridges have been constructed - among these the two longest spans of the 20th century.

Longest cable-stayed bridges

No.	*Name*	*Span*	*Traffic*	*Country*	*Year*
1	Tatara Bridge	890 m	Road	Japan	1999
2	Normandie Bridge	856 m	Road	France	1995
3	Qingzhou Minjiang Br.	605 m	Road	China	1996
4	Yangpu Bridge	602 m	Road	China	1993
5	Meiko Chuo Bridge	590 m	Road	Japan	1997
6	Xupu Bridge	590 m	Road	China	1996
7	Skarnsund Bridge	530 m	Road	Norway	1991
8	Tsurumi Fairway Bridge	510 m	Road	Japan	1994
9	Øresund Bridge	490 m	**Road+rail**	Denmark/Sweden	2000
10	Iguchi Bridge	490 m	Road	Japan	1991

Table 1. The ten longest cable-stayed bridges in the year 2000

The achievements within construction of long span bridges clearly shows that cable supported bridges can be built in a safe and reliable way. However, a few problems still exist regarding

individual cable oscillations and durability of cables. Besides that a continued evolution of design, fabrication and construction methods might lead to improved structural efficiency and further savings in construction costs.

With increasing span lengths the width-to-span ratio will decrease. For cable-stayed bridges this will complicate the commonly used free-cantilevering erection. Consequently, overall design modifications or special stabilizing measures have to be introduced to ensure a safe behaviour in the construction phase and eventually also in the final service condition.

Longest suspension bridges

No.	*Name*	*Span*	*Traffic*	*Country*	*Year*
1	Akashi Kaikyo Bridge	1991 m	Road	Japan	1998
2	Storebælt East Bridge	1624 m	Road	Denmark	1998
3	Humber Bridge	1410 m	Road	UK	1981
4	Jiangyin Bridge	1382 m	Road	China	1998
5	Tsing Ma Bridge	1377 m	**Road+rail**	Hong Kong	1997
6	Verrazano Narrows Br.	1298 m	Road	USA	1964
7	Golden Gate Bridge	1280 m	Road	USA	1937
8	Höga Kusten Bridge	1210 m	Road	Sweden	1997
9	Mackinac Bridge	1158 m	Road	USA	1957
10	Minami Bisan Seto Bridge	1100 m	**Road+rail**	Japan	1988

Table 2. The ten longest suspension bridges in the year 2000

Longer spans result in larger free lengths of stay cables giving more pronounced sag effects and less resistance against individual cable oscillations. To counteract these adverse effects it becomes relevant to consider more elaborate cable systems forming a net composed of primary stay cables and secondary stabilizing cables.

Longer stay cables will complicate their fabrication, transport and erection so improvements become essential. This also applies to the corrosion protection and the surface pattern (to suppress rain-wind induced vibrations).

The truss, traditionally used in many of the longest suspension bridges, is still the natural solution in case of double deck structures. An up-to-date example on this is the Øresund Bridge under construction between Denmark and Sweden. With a length of 490 m the cable-stayed span of this bridge will be the longest to carry both road and full railway loading.

2. Suspension bridges

In the first third of the 20th century the suspension bridges experienced a considerable development as spans grew from 483 m in the Brooklyn Bridge to 1280 m in the Golden Gate Bridge, i.e. an increase by a factor of more than 2.5. The further increase in the 61 years from the Golden Gate Bridge to the Akashi Kaikyo Bridge was 'only' about 1.6.

In their main structural arrangement the suspension bridges have not changed dramatically during

the 20th century. They are still based on a pair of single (or double) parabolic main cables anchored at the ends to anchor blocks and supporting the entire bridge deck (or the main span only) through hangers. The two cable planes are always vertical and positioned above the edges of the bridge deck. The pylons consist of two vertical (or quasi vertical) columns interconnected by struts or by diagonal bracings (Fig.1).

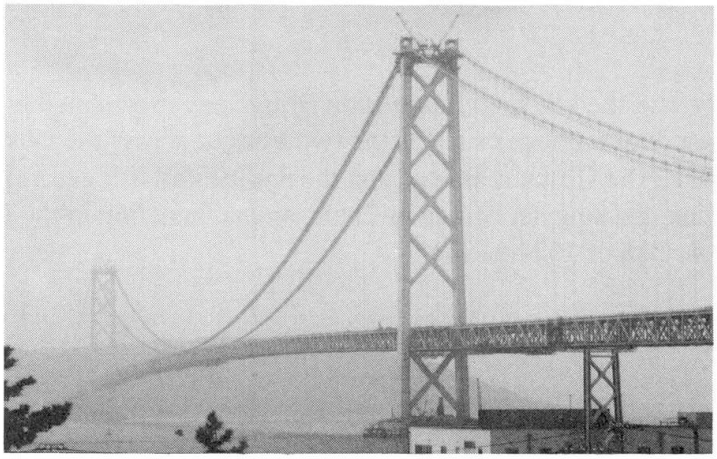

Fig.1 The Akashi Kaikyo Bridge

The most important innovation within suspension bridges in the 20th century is undoubtedly the introduction of the slender streamlined box girder to replace the more bulky trusses which were earlier used to achieve aerodynamic stability. The streamlined box was developed by British engineers and initially introduced during the construction of the Severn Bridge in the early 1960s, Fig.2 and Ref.[1]. The streamlined box is characterized by low weight, easy fabrication and low maintenance cost - the latter especially if the interior of the box is corrosion protected by a dehumidification plant as used for the first time in the Lillebælt Suspension Bridge from 1970, Ref.[2].

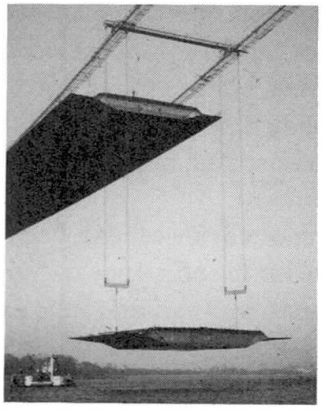

Fig.2 The Severn Bridge under construction in 1964

Traditionally the girders of three-span suspension bridges are separated by expansion joints at the pylons so that the total length from anchor block to anchor block is divided into three simply supported spans. However, in a few cases this arrangement has been substituted by a girder being continuous over the entire length. In a major bridge this was seen for the first time in the Tancarville Bridge from 1959, and later it was also used in the Tagus River Bridge in Portugal and in the Bisan Seto Bridges in Japan. In the latter case the main reason was to eliminate the large angular deflections occurring if expansion joints were positioned at the pylons - a feature of special

importance in these bridges originally planned to be crossed by the high speed trains Shinkansen.

In bridges with a large flexural stiffness of a continuous girder, high stresses will be induced in the region adjacent to the pylons due to the rigid vertical support and the imposed deformations from the distortions of the cable system. In the double deck trusses of the Bisan Seto Bridges it was, therefore, necessary to apply high strength steels with a yield point of 700 MPa in parts of the stiffening truss.

After the Severn Bridge and the Lillebælt Suspension Bridge the streamlined box has been applied in many other major suspension bridges such as the two bridges across the Bosporus in Turkey, the Humber Bridge in the UK, the Ohshima Bridge and the Kurushima Bridges in Japan, the Höga Kusten Bridge in Sweden, the Jingyan Bridge in China, and culminating in the Danish Storebælt East Bridge with a main span of 1624 m, Fig.3.

Fig.3 The Storebælt East Bridge

In the Storebælt East Bridge the girder is continuous from anchor block to anchor block where longitudinal movements are restrained by large hydraulic buffers. In connection with a central clamp on the main cable at midspan this arrangement increases the stiffness under asymmetrical short term loading and reduces the movements in the expansion joints under moving traffic. With its slender box having no vertical support at the pylons the bending stresses remain within allowable limits so normal steels with yield points around 350 MPa have been used throughout. The continuity of the girder has also made it possible to avoid the traditional cross beam between the two pylon legs immediately below the stiffening girder.

Apart from the streamlined box only minor advances have been experienced within the design of suspension bridges. An attempt to increase the efficiency of the hanger system by inclining the cables to form a triangulated cable net has not lived up to the expectations.

In the construction process advances have been seen due to the introduction of welding and large segment girder erection. Cable erection has to some extent been improved by introduction of the prefabricated parallel wire strand (PPWS) method where the wires are pulled across in bundles of typically 127 at a time. However, efforts to improve the traditional air-spinning method have also proved successful so it is not evident which method should be the preferred one in the future.

The developments achieved within the design and construction of suspension bridges with a single box girder has certainly improved its competitiveness, but it has also revealed that this simple concept has its limitation. A number of investigations indicate that with a single box it will be difficult to achieve aerodynamic stability for spans close to 2000 m and even more for spans beyond. However, most of the benefits of the single box, such as low weight, easy fabrication and

efficient maintenance, can still be achieved if the box is split into twin or a triple boxes.

As part of the investigations for a bridge across the Strait of Messina between Sicily and continental Italy a girder with three separate boxes has been thoroughly developed and analysed (Fig.4). This has resulted in a design characterized by an excellent aerodynamic performance despite the extreme span of 3300 m, Ref.[3] and [4].

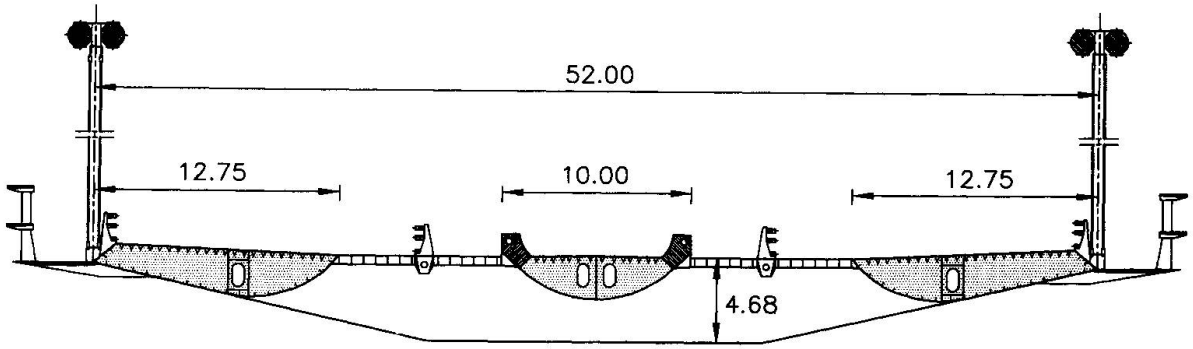

Fig.4 Cross section of the Messina Strait Bridge as developed by Stretto di Messina SpA

The triple box design for the Messina Strait Bridge was developed to allow transmission of a dual-three lane motorway and a centrally positioned double track railway. For pure road bridges a twin box arrangement will be the natural solution if spans go beyond 2000 m.

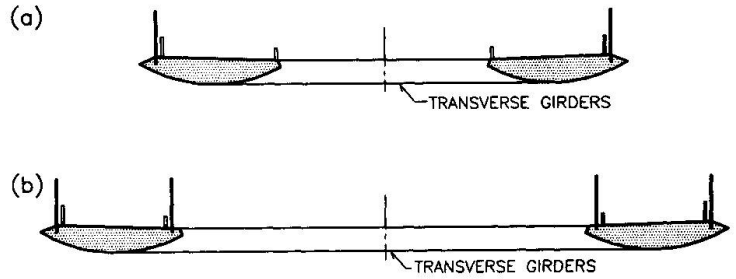

Fig.5 Cross sections of twin box girder decks with two, respectively four cable planes.

The recent investigations into the twin box concept have generally been based on a cross section as shown in Fig.5(a) with the two boxes supported by two vertical cable planes. The favourable behaviour of the twin box concept is linked to the fact that the wide slot between the two boxes reduces the ratio between the twisting and the lifting aerodynamic forces. At the same time the small depth that can be chosen for each of the two boxes results in a low drag.

With a twin box arrangement as shown under (a) with only two vertical cable planes attached to the outer edges of each box it will be required to connect the boxes by transverse girders at every hanger position, i.e. in a distance of 30-40 m. However, if each box is supported by two cable planes, as originally proposed by Richardson in Ref.[5], and shown in Fig.5(b), the vertical loads can be transferred without assistance from the transverse girders. It will, therefore, be possible to limit the number of cross girders to what is needed to safeguard the global aerodynamic stability. The spanwise distance between the transverse girders can then be chosen to many times the distance between the hanger attachments in the longitudinal direction.

Each box with double cable plane support will undoubtedly be aerodynamically stable over a length of several hundred metres so the number of transverse girders can be drastically reduced compared

to the twin box concept with two cable planes and transverse girders at every hanger position. Also, the fact that the vertical loads can be transferred from each box to the cable system without introducing bending in the transverse girders implies that there is a much larger freedom in choosing the width of the slot between the two boxes. Finally it should be emphasized that in the system with four cable planes the erection of each box girder can proceed independently, and that the erection units are more simple and manageable than in the system with two cable planes where all erection units will comprise two boxes and the intermediate cross girder.

The advantages in relation to the transfer of local vertical loads to the cable system and the simplifications regarding erection must, however, be weighed against the increased number of cable planes and the less efficient global torsional support offered by the inner cable planes.

The structural elements of suspension bridges have generally been characterized by an adequate durability if the right materials have been chosen and an efficient maintenance has been made. Thus, several suspension bridges with main cables made of galvanized wires are about to reach - or have already passed - the one hundred year lifetime. For the hangers the durability has been less convincing and many major suspension bridges have had their hangers replaced. Luckily, the replacement of hangers is a relatively easy operation compared to a replacement of the main cables.

To arrive at more durable hanger cables in the Storebælt East Bridge it was chosen to make these cables of fully galvanized locked-coil strands inside an extruded polyethylene sheath. This is expected to give a better durability than with helical bridge strands of round galvanized wires.

It has at several occasions been investigated whether it would be possible to protect the main cables by dehumidification and the system is now tested in full scale in the Akashi Kaikyo Bridge. The results of this test will certainly be of great interest to bridge engineers around the world.

The recent developments in main cable erection and large girder segment erection have improved the competitiveness of the suspension bridge in the span range from 500 m to 1000 m - a range in which cable-stayed bridges started to move into during the 1990s. It is, however, probable that also the degree of imagination put into the design will have a strong influence on the choice of bridge type. New thinking regarding the shape of pylons, anchor blocks and girders could lead to more unique suspension bridges with a different and more exciting appearance (Fig.6). Recent suspension bridge designs are characterized by insignificant variations in the overall appearance - in contrast to cable-stayed bridges showing large variations in the shape of girders and pylons as well as in the configuration of the cable system.

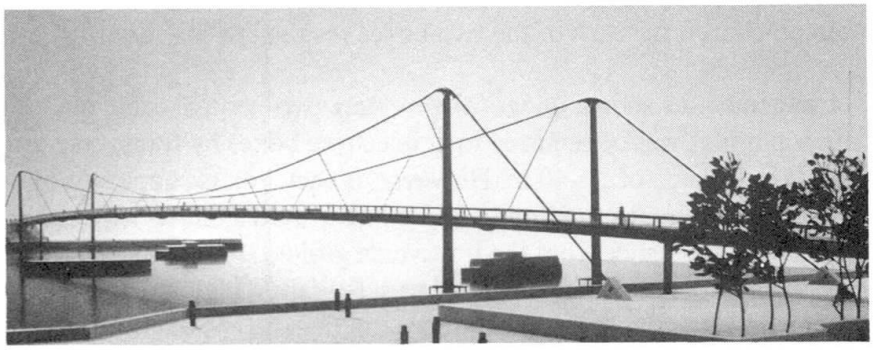

Fig.6 Design for a pedestrian bridge across the Thames in London. Free-standing column pylons with axial compression due to orientation of the backstays in the vertical plane defined by the pylon axis and the adjacent main span cable tangent (Millennium Bridge Competition 1996)

3. Cable-stayed bridges

Cable-stayed bridges have had their entire development taking place in the second half of the 20th century and they are today the preferred solution for road bridges with spans in the range from 200 m to 500 m, but even outside this interval the bridge type has been applied at several occasions.

In contrast to suspension bridges, cable-stayed bridges are built with a large variety of forms and choice of structural materials. In particular the pylons are seen in many different forms - as free standing posts or in A-, Λ-, diamond-shape, etc. The girder can consist of a solid concrete slab, a concrete slab with longitudinal and transverse concrete ribs/I-shaped steel girders, or a box girder in concrete or steel. The cable system can comprise a single central cable plane, two vertical cable planes or two inclined cable planes, Ref.[6].

In some cases the imagination in designing cable-stayed bridges of an unusual appearance has gone too far and led to structures characterized by a somewhat inefficient structural system (Fig.7).

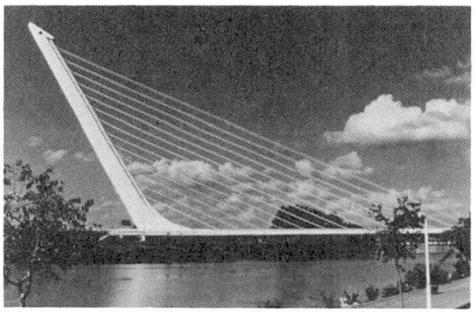

Fig.7 The Alamillo Bridge in Sevilla. The combination of a heavy, leaning concrete pylon and a lightweight bridge deck balances in a clever way the dead load but under traffic load large moments will be induced in the pylon and its foundation

For cable-stayed bridges with spans of medium length and relatively wide girders it will generally be unnecessary to streamline the girder as aerodynamic stability can be achieved even with bluff cross sections. However, when moving into the range of long span bridges, the streamlined box girders as developed for suspension bridges will be required. Recent examples on this feature are the Normandie Bridge (Fig.8) in France and the Tatara Bridge in Japan both with main spans in excess of 850 m.

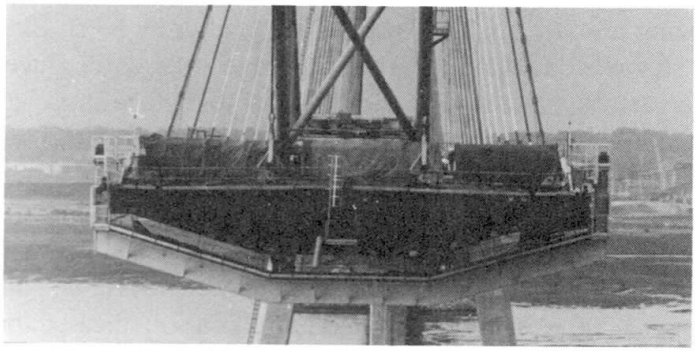

Fig.8 The box girder of the Normandie Bridge

The most troublesome behaviour of cable-stayed bridges is linked to the stay cables themselves either due to individual cable vibrations or to insufficient durability. Among the cable vibrations

especially the rain-wind induced vibrations have given unpleasant surprises, and the phenomenon is still not fully explained and understood despite the research efforts carried out within this field since it was for the first time recognized in the mid 1980s.

At present there is no analytical method available to determine if an actual stay cable is prone to rain-wind induced vibrations but it is known that the phenomenon is linked to the formation of a rain water rivulet on the surface of the stay cable and also that there is an influence of the surface roughness. Thus, from wind tunnel tests it has been determined that a new and clean polyethylene tube is less likely to vibrate than an old and dirty tube.

An efficient way to eliminate the rain-wind induced vibrations is to disturb the formation of the rivulet by adding ribs to the surface of the stay cable. Quite small and discrete ribs can have a pronounced effect in reducing the tendency to rain-wind induced vibrations, as it was clearly illustrated during wind tunnel tests of the stay cables for the Øresund Bridge. Here the 250 mm diameter stay cables were tested with a double helical fillet with a height of only 2.1 mm. Even with these modest ribs the vibrations occurring with the smooth stay cable disappeared.

To suppress individual stay cable vibrations of all categories it has in some cases been tried to add secondary stabilizing cables so that the total cable system is transformed into a cable net. There is, however, at present not a reliable method for designing the secondary cables and their joints to the primary stay cables and as a consequence in some cases breaking has occurred in the secondary cables or their attachments. This breaking is probably due to the high pulsating impact forces induced if the secondary cables are not properly pretensioned. In that case they will be subjected to severe impact forces (slamming) each time the secondary stays is tightened by the displacements of the primary stays. Also, to give a stabilizing effect perpendicular to the cable plane it is essential to have an efficient pretension in all secondary cables.

It has in some cases been tried to improve the efficiency of secondary cables by introducing dampers in the nodes between the intersecting cables, but such a solution should only be used if dampers with a high degree of robustness are available.

At the cable anchorages in the girder and pylons, dampers of different types have been introduced with good results. At these locations it will be relatively easy to install robust dampers and at the same time inspection, repair or replacement can be performed efficiently.

Secondary stabilizing cables are often added to the cable system after installation of all primary stay cables. The secondary cables are then stressed by pulling at the girder level. By this procedure the tension in the secondary stay will diminish from the anchorage at the girder level to the upper stay cable node if the secondary cable is attached to all primary stays before stressing. As a consequence the pretension in the secondary cables will be modest at the top where the stabilizing effect often will be most needed.

To maintain a high and constant tension along each secondary cable it is necessary to stress it against the topmost stay cable. This implies that the upper stay cable will be pulled down and characterized by an increased sag, as shown in Fig.9. Here it is also indicated that the secondary stabilizing cables conveniently should be straight from the top stay cable to the girder and be oriented perpendicular to the top cable.

With the arrangement shown in Fig.9 there will be no force transfer in the dead load condition from the secondary to the primary cables at the intersections - except at the top cable. The nodes

between the primary and the secondary cables will be easiest to arrange if the secondary cables consist of two strands passing on either side of the stay cables. In that case the joint can be composed of three clamps, one large and two smaller, connected in such a way that they can be mutually rotated around a horizontal axis. This will allow the joint to be used at all intersections between cables having the same diameter of primary and secondary cables. Furthermore, by keeping the outer clamps untightened during tensioning of the secondary cables it is ensured that the pre-tension will be constant from deck level to the top stay cable.

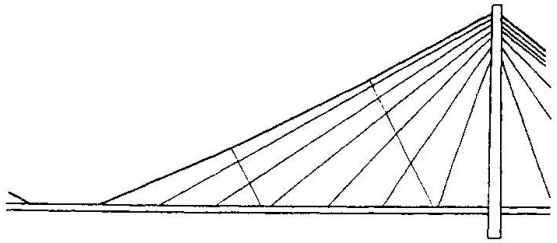

Fig.9 Secondary stabilizing cables stressed against the top stay cable

During the 1980s a number of cable-stayed bridges have had their original stay cables replaced due to insufficient durability leading to corrosion and wire breaks. Efforts have consequently been made to improve the durability and it is today regarded as imperative to have a double barrier protection against corrosion, e.g. by using galvanized wires inside a polyethylene sheath or a tube filled with a corrosion inhibiting substance.

The developments in fabrication of stays with increased durability have undoubtedly prolonged the lifetime, but it has also led to cost increases. Together with the cost of different measures to increase the aerodynamic stability this has resulted in unit prices for erected and protected cable steel in cable-stayed bridges being 1.5-2 times larger than for cable steel in suspension bridge main cables. This influences the competitiveness of cable-stayed bridges in the upper span range. So at present it seems as if a further prevalence of cable-stayed bridges in the span range above 500-600 m will depend on the development of new efficient and reliable methods for stay cable manufacture, corrosion protection, erection and stabilization against vibration of individual stays.

The competition between suspension bridges and cable-stayed bridges will of course also be much influenced by the way in which each bridge type's special advantages can be utilized in an actual case. For the cable-stayed bridges the decisive advantages are the superior rigidity of the global structural system and the self anchoring of the cable system (excluding the need for large anchor blocks)

4. The Øresund Bridge

The overwhelming part of all cable-stayed bridges constructed in the second half of the 20th century are for road traffic only. However, in a few cases this type of bridge has also been built to transfer train traffic. Among these bridges the Øresund Bridge stands out as it does not only have the longest span, 490 m, but also is designed to allow passage of freight trains with a unit weight of 80 kN/m on both tracks (simultaneously) or of passenger trains with speeds of up to 200 km/h.

The design of the Øresund Bridge originated in the spring of 1993 when the ASO Group prepared a design for the competition announced by Øresundskonsortiet with the purpose of selecting a

consulting engineer to assist the client in the following phases. All the main innovations of the Øresund Bridge design appeared during the period when the competition design was prepared for a double deck bridge with road and rail traffic at two different levels. After the competition when the design of the ASO Group had been selected to be carried further the whole concept was once more evaluated in all its features but it was found that the original concept was so consistent in its main concept that only a few minor refinements could be made. Also in the following phases of tendering and detailed design by the contractor and his consultants all the main features of the original competition design remained unchanged.

The bridge constituting the eastern part of the Øresund Link has a length of 7.8 km and consists of three main sections: the western approach bridge with a length of 3014m; the main bridge (at the navigation channel) with a length of 1092m; and the eastern approach bridge with a length of 3739m.

With the main bridge forming a relatively small part (~ 15%)of the total bridge length it was obvious that a structural solution should be sought where the approach spans (comprising continuous trusses), could form a part of the main bridge without a complete change of structural system and materials, and without an abrupt visual transition. Also the strict requirements regarding strength and stiffness imposed by the passage of both heavy freight trains and highspeed passenger trains had a strong influence on the design of the main bridge.

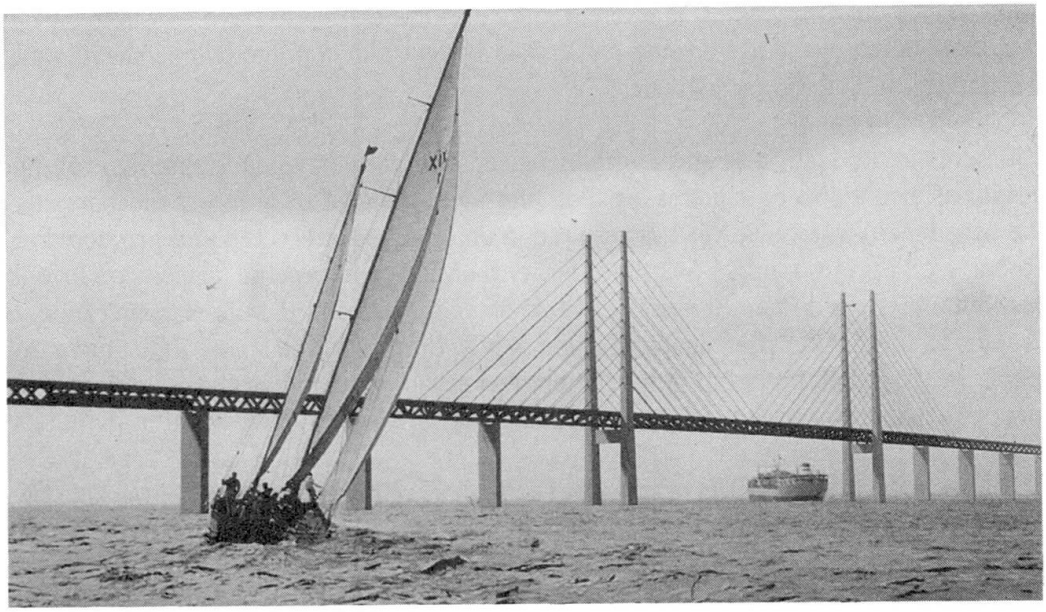

Fig.10 Artist's impression of the Øresund Bridge

All these requirements clearly pointed towards a cable-stayed main span with a girder composed of steel trusses and an upper concrete deck as in the approach spans of the bridge. The demand for a high degree of rigidity led to a harp-shaped cable system with relatively steep cables and intermediate support in the side spans, as illustrated in Fig.10.

In accordance with the original competition design the symmetrical truss geometry with all diagonals of the approach spans having the same length in is adjusted so that in the cable supported regions the two diagonals leading to each node have different inclinations and lengths. This allowed the long diagonals to have the same direction as the stay cables. The transition from diagonals forming equilateral triangles to 'skew' triangles is made by increasing the distance

between two of the top chord nodes in one bay from 20 m to 25 m, as it is seen in Fig.11. At the botom chord the node distance is kept at a constant 20 m even at the transition point.

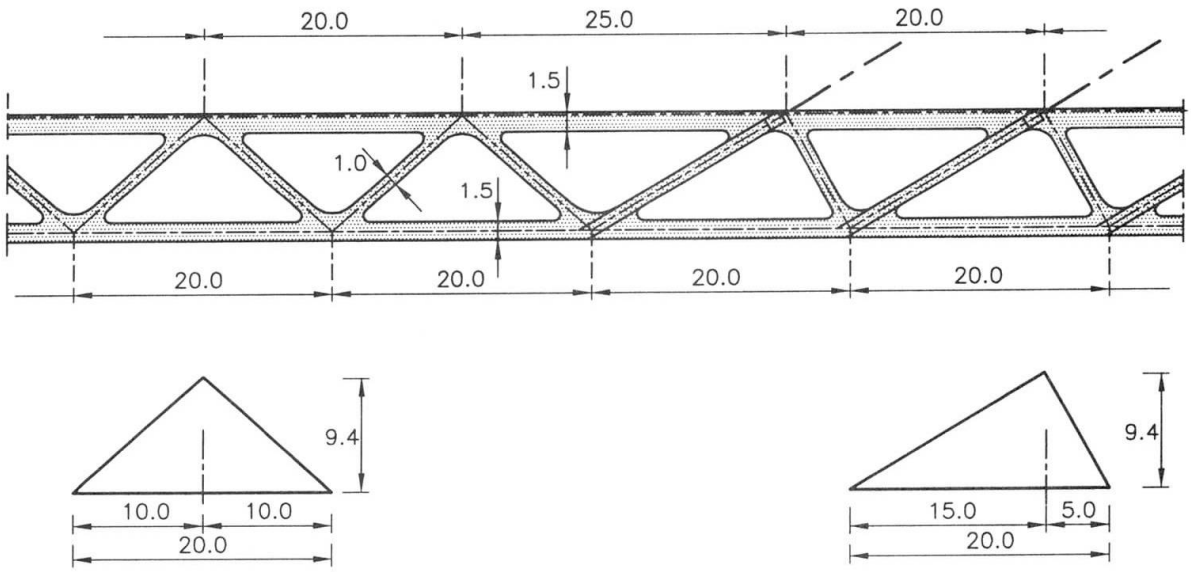

Fig.11 Change of truss geometry

The two vertical cable planes are spaced 30.5 m apart, i.e. with the cable centre lines 3.5 m from the edge of the 23.5 m wide bridge deck. This position was chosen to allow the vertical cable planes to be moved out so that they could coincide with the vertical centroid of the pylon legs. That made it possible to avoid any cross bracings between the two pylon legs above the bridge deck despite the fact that the pylon was to be made of concrete, Fig.12. Excluding cross bracings not only influenced the appearance in a favourable way but also simplified the casting of the upper part of the pylon.

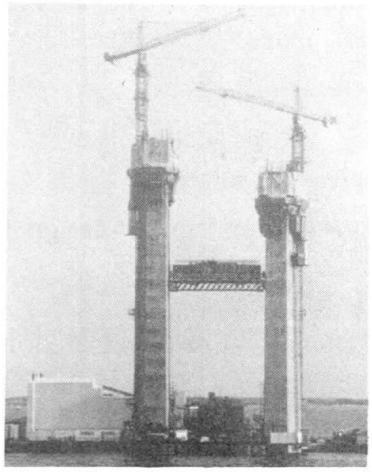

Fig.12 The pylon of the Øresund Bridge under construction in early 1998

With the cable planes moved out from the edges of the upper roadway deck with its overhang, it became necessary to add special structural elements to transfer the stay cable forces to the main trusses. Triangular latticed brackets ("outriggers") were consequently positioned outside the main trusses in the same inclined plane as the long diagonals, Fig.13.

The triangular outriggers and the adjusted truss geometry give the main span of the Øresund Bridge a quite unique appearance and at the same time it exhibits an honest structure where nothing is done to hide the flow of forces from the two decks to the stay cables and further to the

203 m high pylons.

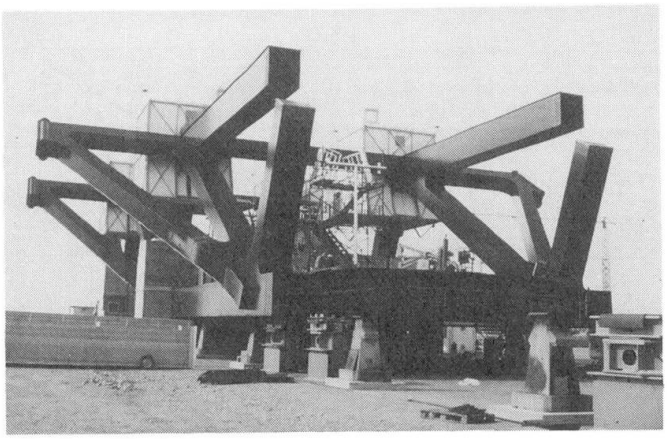

Fig.13 Truss element for the cable-stayed portion of the Øresund Bridge

Acknowledgements

The Øresund Bridge is being built by **Øresundskonsortiet** - a limited company with the Danish and the Swedish State as the only shareholders.

Consulting Engineers for the bridge: ASO Group, comprising Ove Arup & Partners, UK; Setec, France; ISC, Denmark and Gimsing & Madsen, Denmark + Architect: Georg Rotne

Contractor: Sundlink Contractors HB, comprising Skanska AB, Sweden; Hochtief, Germany; Højgaard & Schultz A/S, Denmark; and Monberg & Thorsen A/S, Denmark. The contractor's consulting engineers: COWI, Denmark and VBB, Sweden

References

[1] G.Roberts, The Severn Bridge - A new principle of design, Proceedings of the International Symposium on Suspension Bridges, Lissabon 1966

[2] Schülein,E.H. & G.Haas: Air-dehumidification in a box girder bridge, IABSE Journ. J-4, 1977

[3] Brown,W.C. & S.Craig: Recent developments in design of suspension bridges, Proceedings of the International Conference on Bridges into the 21st Century, Hong Kong 1995

[4] Brown,W.C.: Development for the Deck for the 3300 m Span Messina Crossing, Congress Report IABSE 15th Congress, Copenhagen 1996

[5] Richardson,J.R.: Aerodynamic Stability of Twin Suspension Bridge Concept, Congress Report IABSE 12th Congress, Vancouver 1984

[6] Gimsing,N.J: Cable Supported Bridges - Concept and Design, Second Edition, John Wiley and Sons, Chichester 1997.

Aerodynamic Design of Very Long-Span Suspension Bridges

Giorgio DIANA
Professor
Politecnico di Milano
Milan, Italy

Federico CHELI
Professor
Politecnico di Milano
Milan, Italy

Alberto ZASSO
Researcher
Politecnico di Milano
Milan, Italy

Andrea COLLINA
Researcher
Politecnico di Milano
Milan, Italy

Stefano BRUNI
Researcher
Politecnico di Milano
Milan, Italy

Summary

New deck design and new kinds of structures have been developed in order to increase the stability and the performances of super long-span bridges allowing very long spans which only some years ago were thought not to be reached. On the other hand, to reach these results, numerical and experimental methods must be available in order to assess the good performance of the bridge subjected to turbulent wind. The paper outlines the different solutions for controlling bridge stability and describes the different methods available for evaluating the response of the structure to turbulent wind.

1. Introduction

In the last decade several long-span suspension bridges have been designed: some of them have been already built, such as Great Belt and Akashi, reaching a maximum span length of 2000m. Some other projects are related to bridges with a span length greater than 3000m (Gibraltar 3500m, Messina and Sunda straight crossings, both 3300m): from this point of view the 21th century can be considered the age of the "over 3000m" span bridges. The increase of span length from 2000m to 3000m is not feasible with a simple extrapolation of the existing bridges, since the structural typology of the bridge must undergo important modifications. The fundamental problem that must be solved in the design of a super long suspension bridges is the aeroelastic one, that is the behaviour of the structure in turbulent wind conditions. The aeroelastic stability of the bridge must be ensured above the design wind speed, ranging from 60 to 80 m/s. As an example, for the Great Belt, with a span length of 1680m, the selected design wind speed was 60 m/s, while for the Akashi Bridge, a value of 78 m/s was assumed. As will be discussed in the following, in order to increase the span length over 3000m, critical speed requirements cannot be satisfied using nor the Great Belt's typology (traditionally suspended single box girder) neither the Akashi's one (traditionally suspended truss girder). Several ways can be followed in order to increase the span length without compromising the aeroelastic stability of the structure, anyone of those implying a reconsideration of the three parameters affecting the aeroelastic stability:

i) Torsional vs. flexural frequency ratio r_f.

ii) Ratio r_t between structural stiffness and equivalent stiffness due to aeroelastic effects.

iii) Total amount of damping, including structural and aeroelastic contributions.

All these parameters must be as large as possible in order to increase the bridge stability. An increase of the r_f ratio implies a modification in the design of the structure; in order to increase the r_t ratio, besides structural modifications affecting the structural stiffness, the shape of the deck must be modified, in order to reduce the aerodynamic forces. The total damping of the structure could be increased in several ways: by means of dynamic absorbers, passive aerodynamic damping devices or even active control. In conclusion, in order to assure the feasibility of extra long suspension bridges the following topics must be carefully analysed:

a) Bridge structural design.

b) Aerodynamic deck design.

c) Adoption of active and/or passive control.

All these ways have been investigated by designers and researchers, whose efforts are aimed to demonstrate the feasibility of bridges with span length greater than 3000m. On the other hand, in order to compare different bridge solutions in the design stage, a tool able to evaluate with accuracy the response of the bridge to turbulent wind and to check its aerodynamic stability is necessary. In this work the approaches usually adopted for the three a), b), c) above mentioned tasks are described, with reference to both existing projects and preliminary studies for future realisations. Moreover, the available methods for the analysis of the response of the bridge to turbulent wind will be described, and their advantages and limits will outlined. The paper is organised as follows:

i) Description and critical analysis of the different strategies for increasing the stability and/or the span length of suspended bridges.

ii) Discussion of the available methods for simulating the structure response to turbulent wind (r.t.w.).

iii) Concluding remarks.

2. Structural-Aerodynamic Solutions

As already mentioned in the previous paragraph, one of the most challenging problem to solve in super long-span bridge design is the aeroelastic stability at design wind conditions. The experience gained on the recently built record span bridges Great Belt East Bridge and Akashi Kaikyo Bridge, together with the parametric analysis considered in the preliminary Gibraltar project (Astiz 1993), showed that the static system of the classical suspension bridges and the modern streamlined single deck box girder solution (Humber, Bosporus, Great Belt) reach an intrinsic limit for spans approaching 2000m (Astiz 1996, Miyata 1993). The fundamental reason is the higher trend of reduction of the first torsional frequency ω_t compared to the flexural one ω_f versus span length, as shown in Figure 1, where the frequency ratio $r_f=\omega_t/\omega_f$ changes from $r_f=3.5$ for main span length $L_s=1000$m to $r_f=2.8$ and $r_f=1.3$ for $L_s=2000$m and $L_s=3000$m. Being in fact the aerodynamic forces quite significant, due to the lifting characteristics of a shallow streamlined box girder, the structural torsional stiffness becomes too low compared to the equivalent aerodynamic one, lowering in this way the critical wind speed. A first attempt is then to increase the flutter speed by various minor structural modifications of the basic solution, having the common purpose of rising the structure stiffness. An interesting sensitivity analysis (Astiz 1993) shows the effects achievable by this approach (see Figure 2). If moderate stability performances are required, as in the Great Belt case (1624 m span and 60 m/s design flutter limit), an optimum compromise of low drag, low vortex shedding excitation and sufficiently high girder torsional stiffness was obtained using a standard design box girder with minor aerodynamic refinements, and structure efficiency improvements. On the other hand the Akashi project showed that the

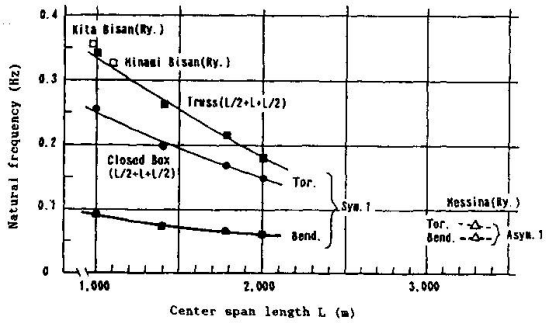

Figure 1 Trend torsional vertical freq. ω_t, ω_f versus span length (Miyata 1993)

Design change with respect to basic solution	Increase in critical velocity (%)
Girder weight (+25%)	+1.1
Distance between cables (+17%)	-8.8
Cable sag (from 1/9 to 1/8)	+2.5
Girder torsional stiffness (+50%)	+11.1
Additional stay cables	+9.1

Figure 2 Effects of structural changes on the critical wind speed (Astiz 1993)

higher flutter limits (78 m/s design critical wind speed) and the 2000m record span length required substantial modifications. The solution was again the attempt to face flutter, maintaining the traditional cable static scheme, through a very rigid and massive truss-box girder, with the final well-known choice of the truss solution (Miyata 1993). On the other hand the lesson

learned with the thorough analysis of a large number of different deck solutions in the Akashi design is that it's not possible to rely only on the girder stiffness and mass increase when the span length reaches or exceeds 2000m, and more substantial geometrical-structural changes are needed, or new ideas have to be developed in the aerodynamic design. Incidentally, it helps to mention that, whatever is the effort, the girder contribution to the bridge torsional stiffness becomes negligible when the span is beyond 2000m, due to the prevailing main cable effects. It needs also to be highlighted that a substantial contribution to the aeroelastic stability of Akashi came also from aerodynamic countermeasures like the adoption of a vertical plate-like stabiliser, the optimal position of the inspection ways, and the longitudinal gap in the deck between the two roadway flat plates. If the only structural way is followed, super long suspension bridges have to abandon the traditional static cable system. Crossed hanger system, or a combination of cross stay (vertical) and horizontal stay (Miyazaki 1997), are a first minor modification aimed at rising the bridge torsional stiffness, allowing a not negligible improvement of the critical wind speed (Astiz 1993, 1996). The greatest improvement in torsional stiffness is achieved through the one cable system proposed in (Leonhardt 1968) (Figure 3) and its variants like the three cable system (Astiz 1996), having on the other hand several drawbacks as great load oscillations in the hangers and pronounced pendulum behaviour. Another interesting scheme is the four-cable system requiring on the other hand a quite complex vertical crossed hanger net to realise an effective improvement of performances in terms of torsional stiffness and critical wind speed (Astiz 1996).

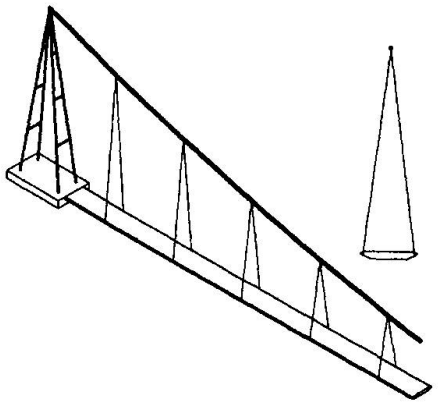

Figure 3 Mono cable system (Astiz 1996)

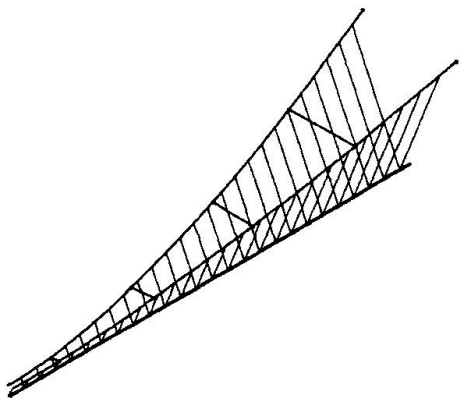

Figure 4 Spatial system with high lateral and torsional stiffness (Gimsing 1997)

The idea of the four cable system was suggested also for the Messina project in (Musmeci 1971) first and in (Borri 1992) later, combined with an hybrid cable-stayed/suspension structure aimed substantially at reducing the total span of the suspension bridge. It has to be noticed however that the lower cables system, adding significant weight to be supported by the overhead main cables, penalises this solution, considering that one of the main advantage of spatial cable systems should be the increase in torsional stiffness avoiding heavy and massive structures. Several authors finally proposed various solutions of spatial cable systems, and the state of the art of this topic is well referenced in (Gimsing 1997). A final spatial solution proposed by Gimsing is shown in Figure 4, combining the advantages of rising both lateral and torsional stiffness of the structure, but requiring very complex tower arrangement and not easy construction procedure. Several authors made parametric comparison of those different solutions, comparing their flutter limits for equal aerodynamic and structural deck characteristics, selecting usually as a reference a standard streamlined box girder and showing for all of them a substantial advantage, with respect to the traditional static scheme (Ito 1996), (Gimsing 1994), (Walther 1994), (Nomura 1994). As previously mentioned, although the central idea to increase the torsional stiffness through a new spatial cable system is conceptually very effective, nevertheless several drawbacks are involved, especially the complexity of the construction stage and the need of developing new not experimented construction technologies, never experienced up to now. It has to be stressed finally that the geometrical complexity of those solutions and the stiffening effects of differently arranged crossed hangers results generally in a quite complex structure dynamic behaviour with structural coupling of vertical and torsional mode shapes. Follows the impossibility

to use a simple 2 D.o.F. modal flutter analysis, as in the well experienced standard suspension bridge scheme, making mandatory at least a multimodal flutter analysis to assess the structure stability limits, as well as a careful check of static divergence. A completely different solution for the aeroelastic stability of very long-span suspension bridges could be that of tuning the two frequencies ω_t and ω_f to the same value. In fact, assuming a modal 2 D.o.F. scheme representative of the aeroelastic bridge behaviour, it is easy to show that making the torsional frequency deliberately equal to the vertical one (and controlling this ratio for all the possible coupling modes), the reduced critical velocity goes to infinity, inverting the trend where flutter speed is usually decreasing with r_f (Dyrbye 1997). In such a case the bridge stability should be generally discussed just in terms of static divergence. On the other hand, similarly to the over mentioned non standard-geometry solutions, no example exists of significant structure designed and built following this idea, not only due to the conservative approach still now followed in the final design choices, but also due to the very dangerous drawbacks of possible static divergence accompanying the low torsional stiffness solutions. The feasibility of some proposed solutions of super long suspension bridges is in fact clearly arguable in terms of torsional static divergence or too large lateral-torsional displacements as in the case of the 2-box and 1-box combined girder recently proposed in (Ogawa 1997) showing torsional rotation in the order of 8 Deg at the wind flutter limit of 70 m/s. Adopting a purely structural approach, a final solution to the aeroelastic stability of very long suspension bridges could rely on composite very light materials. As mentioned in (Ostenfeld 1992) and (Meier 1991), the availability of Carbon Fibre Reinforced Polyester (CFRP) with tensile strength of 3300 MPa and density of 1.56 kg/dm^3 (compared with 1700 MPa and 7.8 kg/dm^3 for steel) could be reasonably affordable in the next future at a competitive price for very long main span length, allowing to build very light structures, having a considerably higher ratio payload/unit mass of cable. Although the E modulus of CFRP is slightly lower compared to steel (165000 MPa compared to 205000 MPa), the use of CFRP supposed limited to the main cable, can reduce considerably the total dead load of the structure and rise the equivalent vertical and torsional structure stiffness and frequencies. On the other hand the main cable-mass penalising effects (in terms of low torsional/vertical frequency ratio), due to the high equivalent torsional inertia, can be reduced, and the relative contribution of high stiffness girder can be more significant. Figure 5 shows the parametric dependence of the critical flutter speed on the structure specific weight, assuming unchanged all the other parameters and in particular the tension in the main cables, the structure equivalent stiffness and the aerodynamic derivatives. The increase of the flutter velocity is due in this case to the higher aerodynamic damping associated with the increase of the natural frequencies caused by the lower structure inertia. All the previous analysis were made considering unchanged the deck

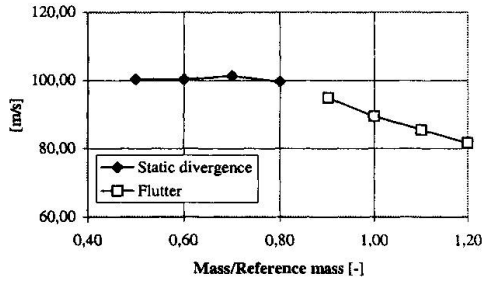

Figure5 Flutter limit as a function of relative modal mass; (Messina bridge)

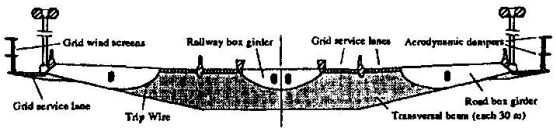

Figure 6 Messina multi-box deck section

aerodynamic characteristics, and examining the only structural solutions to the problem of controlling the aeroelastic instability of very long suspension bridges. On the other hand this is a purely academic exercise, as the aerodynamic improvement of the section is always a tool available for the designer. A complementary approach to the problem is in fact the attempt to reduce the ratio Aerodynamic/Structural forces working on the refinement or on innovative aerodynamic design of the structure. The history of the design experience of the two significant projects, the first already built (Akashi), the second developed up to a definitive stage (Messina), shows in fact that for span length over 2000m, the reduction of the aerodynamic deck lifting characteristics and the use of some aerodynamic damping became mandatory. Having as a target the optimum deck aerodynamic design, four fundamental objectives should be pursued. (a) Low

lifting characteristics (low lift and moment derivatives). (b) Low drag. (c) No significant vortex shedding excitation. (d) High aerodynamic damping. In the opinion of the authors, having as a target main spans over 2000m a successful design must search a compromise solution between the four over mentioned objectives. On the other hand, as shown by both Akashi and Messina projects, the adoption of a "slotted" deck solution seems to be unavoidable if low lifting characteristics are searched. While in the Akashi case the solution was a traditional flat plate, supported by a single truss girder and interrupted by a large gap at mid-chord, the Messina project adopted the new idea of multi-box girder, with three highly streamlined longitudinal box girders connected by box-shaped cross girders at 30m distance (Figure 6). Open grids in the areas between the longitudinal and transverse box girders allow pressure equalisation between upper and lower side of the deck, reducing the lifting characteristics of the section. Great advantage of the Messina solution is the possibility of maintaining an overall section streamlined profile with extremely low drag (if compared to Akashi as an example) together with very low vortex shedding excitation. The Messina deck section is on the other hand an example of optimum compromise between the four over mentioned aerodynamic design objectives: as an example, a careful experimental investigation allowed to select the optimum wind barriers porosity giving low drag, effective traffic sheltering, unchanged aerodynamic characteristics between no traffic-full traffic conditions, as well as effective performances of wing shaped aerodynamic dampers integrated in the wind barriers (Diana 1993). The Messina experience showed as a conclusion that, for very long-spans, the multi-box deck solution is the most promising in terms not only of optimum aerodynamic design, but also of light weight of the structure, easy maintenance and modularity construction technology, requiring on the other hand a very careful aerodynamic refinement, in order to control flow separation and allow uniform performances in a wide range of wind angle of incidence (Brown 1996).

Following the design strategy of taking advantage of high aerodynamic deck performances, it becomes of crucial importance the assessment of the right aerodynamic characteristics of the section and the availability of very reliable mathematical models simulating the aerodynamic stationary and non stationary wind effects. As far as concern the first issue, wind tunnel techniques are still an unavoidable step in the design stage: the most critical aspects of such experimentation is the consistency of scale model data with the real full scale behaviour of the structure, as well as the development of numerical-experimental techniques allowing to simulate correctly the turbulence effects on the bridge stability and the non-linear effects associated with high angle of incidence, as will be better explained in the next paragraph.

The possibility to approach the aerodynamic forces not only as a non conservative destabilising field, but also as a possible source of damping for the structure, is on the other hand the very last issue in very long-span bridges aerodynamic design, already experienced in terms of passive solutions, but investigated and considered as applicable also in terms of active control. As far as concern passive aerodynamic damping, several solutions were proposed (Cobo del Arco 1997), (Zasso et al. 1993b) most of them consisting in wing profiles fixed at the section leading or trailing edge zone, adding torsional and vertical direct damping, but increasing also the crossed terms. It's clear that the solutions applicable in a true project must take into account feasibility problems, being again a compromise between the requirements of maximum effectiveness (free stream) and the practical realistic proposals on how to integrate the aerodynamic damper in the overall deck section.

The final tool never applied in real structures, but already considered by several authors in a feasibility stage is the active control (Miyata 1996), (Achkire 1997), (Cobo del Arco 1997). High performance wings in the undisturbed leading and trailing edge are the most effective tools, and a very reliable numerical model simulating the overall deck section aerodynamics together with the global bridge dynamics is then mandatory in order to run the active control in an effective way. In the opinion of the authors, even though very attractive results are devised, this solution is still a research topic, due to the reliability requirements of structures like the civil-transport ones. For safety reason, is difficult to believe that a structure collapsing at a wind speed lower than the design one, if abandoned to its passive resources, could be approved in the next future. In other words the structure must be intrinsically stable and the active control should be used only for increasing the overall performances as an example in terms of comfort, rail and road runnability, fatigue life-expectance of the structure.

3. Models for the Simulation of Bridge Response to Turbulent Wind

In order to define in quantitative terms the effectiveness of different design solutions, a tool allowing the evaluation of all the different aspects of the aeroelastic problem (i.e. bridge buffeting and aeroelastic stability) is needed. At the different stages of the design process, depending on the level of accuracy required, the aeroelastic analysis of a long-span bridge can be performed using methodologies of different complexity. As an example, the tools adopted in the initial stage of selection and optimisation of the structural typology, where repeated calculations are needed, are different from those that must be used for the final check of the optimised solution, where high accuracy is needed. Figure 7 shows the aeroelastic analysis procedure usually adopted: in the left section the typology optimisation process is described, while in the right section the final check procedure is outlined. The paper will not describe in detail the mathematical models used in the optimisation stage, where consolidated linear approaches are adopted, using section model experimentally measured flutter derivatives and modal reduction of the structure degrees of freedom (Scanlan & Tomko 1971, Scanlan 1992). These approaches are affected by the approximations implied by the linearity assumption, where in fact the system shows a non-linear behaviour, especially under the action of turbulent wind, where high variations in the angle of attack occur (Miyata et al. 1995, Bocciolone et al. 1990).

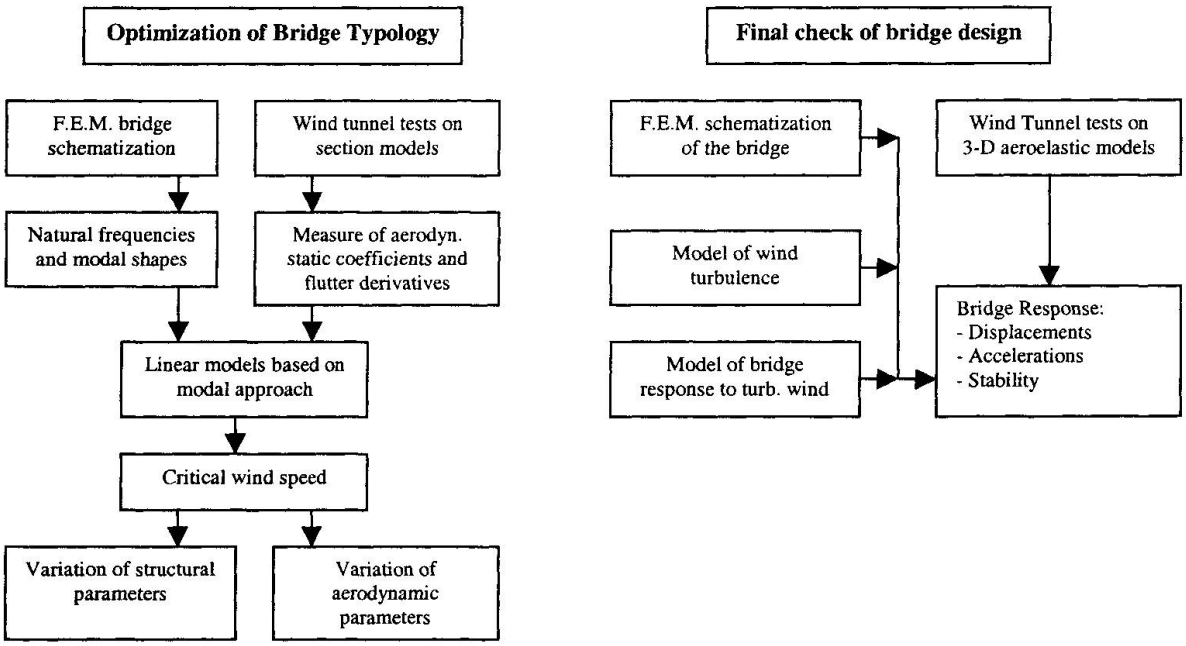

Figure 7 Procedures for the aeroelastic analysis

Nevertheless, the critical wind speed values estimated by linearised methods are generally reliable, as far as traditional typologies of single span bridges are concerned. As already mentioned, when dealing with non traditional typologies like those using crossed hangers (Astiz 1996) or horizontal stay ropes (Gimsing 1997) or bridges with very close main cables (Ogawa et al. 1997), modal approaches based on coupling of a single flexural mode and a single torsional mode should be carefully considered. For these structures multi-modal approaches are in fact recommended as the flexural modes shape is usually different from the torsional one and sometimes it is not possible to make a clear distinction between flexural and torsional modes, showing each mode both components of motion. In the same way, the procedure of superimposing the effects of the mean wind speed and the effects of wind velocity fluctuations, as done in (Ogawa 1997) should be regarded with particular care. In Figure 7 right section, the two main approaches available for predicting the real bridge behaviour, the numerical one and the experimental one, are reported. The numerical approach consists in the artificial generation of a space-time distribution of wind speed and subsequently in the simulation of the bridge r.t.w. using a finite element model of the structure in conjunction with an appropriate non-linear model of the aeroelastic forces. On the other hand the experimental approach consists in wind tunnel tests on complete

tridimensional aeroelastic bridge models (Reinhold et al. 1993). Both the analytical and the experimental method, reproducing the real bridge behaviour, allow to estimate the bridge dynamic response, and in particular the mean values (static response), the r.m.s. values and the spectra of vertical and torsional deck motion excited by the turbulence (buffeting response). From these data it is then possible to evaluate the wind induced modifications of the damping ratio and of the natural frequency of each mode of the structure, as a function of the wind speed (Diana et al. 1995, Sumiyoshi et al. 1993). From the trend of flexural and torsional frequencies (Figure 8), and damping ratios (Figure 9), the instability threshold can be obtained. From this figure it can also be defined the stability index of the bridge: in this case, at 62 m/s design wind speed, the stability index is 4%. The static stability and buffeting problem are then considered simultaneously. The two approaches are not in contrast each other, and in fact they can be considered as complementary and sometimes have been used in conjunction.

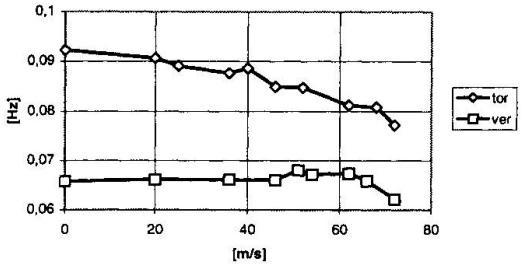

Figure 8 Effect of wind speed on the first flexural and torsional frequencies for 1:250 model of Messina Bridge

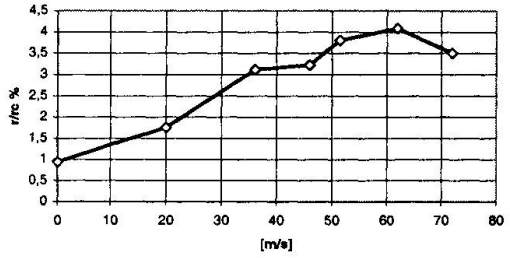

Figure 9 Effect of wind speed on the damping ratio of the first torsional mode, 1:250 model of Messina Bridge

3.1 Wind Tunnel Tests on Full Aeroelastic Models

Being the techniques adopted in these tests well established, the discussion will be limited to the description of the advantages and disadvantages of this method. In particular among the main advantages the following ones can be mentioned:

- It is possible to reproduce the features of the problem in its entirety, including turbulence effects, tridimensional and non-linear effects.
- The aeroelastic model measured response can be used to verify and tune a numerical model of bridge r.t.w., being in this case easy to characterised thoroughly the process input and output i.e. the wind speed field, and the model motion.

The weak point of this experimental method can be summarised as follows:

- It is not easy to reproduce in the wind tunnel the real wind turbulence distribution, and in particular the correct ratio between the integral length of turbulence and the characteristic dimension of the model (e.g. the chord length).
- Scale effects, related to the difference between full scale and test conditions Reynolds numbers. The scales usually adopted for aeroelastic models range from 1:300 to 1:100 (or less in few cases), depending on the available wind tunnel facilities. This effect can be monitored measuring the flutter derivatives of different scale section models (Zasso 1993a).
- It is not always simple to accurately reproduce on the scale model the natural frequencies, modal shapes and damping ratios of the real structure.

Anyway this method has to be considered an indispensable tool for verifying the aeroelastic behaviour of a long-span bridge, although being very expensive and time consuming, and therefore it must be considered the conclusive step of the design process.

3.2 Methods for the numerical simulation of bridge buffeting

There are two main approaches to the problem of simulating the bridge response to turbulent wind, the first usually named "frequency domain approach". In this approach the input is represented directly by the statistical properties of the wind (Power Spectral Densities of the wind speed components and coherence functions along the bridge) and the output is represented by the

statistical quantities (e.g. P.S.D.) describing the motion of the structure. This approach is inherently linear: in its more sophisticated formulation the "self excited" component of the aerodynamic forces (that is the component due to the motion of the structure) is represented through the flutter derivatives evaluated in correspondence of a reference static condition assumed "a priori". For this reason this approach cannot be considered adequately accurate for the final check of the aeroelastic behaviour of a long-span bridge. The method analyses separately the static response of the bridge, the stability and the buffeting response.
The second approach, which will be called in the following "time domain approach", consists into two main steps: first a space-time wind distribution is artificially generated from the knowledge of the wind basic statistical properties; as a second step, the numerical integration of the structure motion equations is performed in the time domain, obtaining the bridge motion as output. The different techniques adopted for space-time wind distribution generation will not be discussed here, it is only mentioned that, as an example an ARMA model, or a wave superposition method can be adopted (Bocciolone et al. 1990, Shinozuka 1972). The dependence on the gust size, with respect to the deck size, is taken into account by multiplying the basic wind spectrum for the aerodynamic admittance function, obtaining the corrected target spectrum, used for wind generation. A question that should be investigated is whether the turbulence coherence is also representative of the coherence of the aerodynamic forces along the bridge: some authors found that the transversal coherence of the aerodynamic forces at different locations is greater than the one calculated on the basis of the wind coherence function (Larose 1997). Before analysing the possible time domain simulation techniques, it is useful to introduce the problem of modelling the aerodynamic forces, representing the crucial point for the bridge r.t.w. simulation.

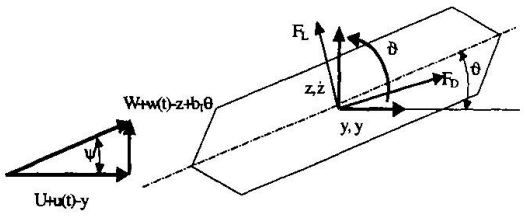

Figure 10 Variables defining wind forces on the deck

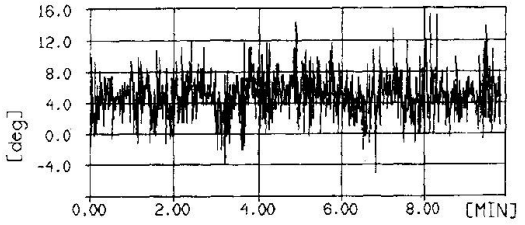

Figure 11 Incidence angle of wind speed measured on Humber bridge, from (Bocciolone et al.)

To this end we will concentrate on a section of the bridge, whose position along the deck is introduced through the spatial co-ordinate ξ: the problem in its essence consists in accurately reproducing the aerodynamic actions on the structure, due to the combined effect of incident flow turbulence and bridge motion, as shown in Figure 10, where U, $u(\xi,t)$ represent respectively the mean value and the fluctuating component of horizontal wind speed, and W, $w(\xi,t)$ are the corresponding vertical components. Moreover y, $\dot{y}$, z, $\dot{z}$, ϑ, $\dot{\vartheta}$ are the parameters describing the deck motion and F_y, F_z and M_θ are the components of the aerodynamic forces. These forces can be considered as the output of a model reproducing the aeroelastic behaviour of the deck, and are non-linear functions of the input quantities U, $u(\xi,t)$, W, $w(\xi,t)$, y, $\dot{y}$, z, $\dot{z}$, ϑ, $\dot{\vartheta}$. In order to experimentally characterise these forces, suitable wind tunnel tests should be carried out on section models, moving the model according to a pre-defined law of motion and introducing controlled components of turbulence in the air flow. Through this kind of tests a model of the wind actions on the deck could be implemented as a "black box" input-output non-linear relationship, for instance by means of NARMAX techniques or neural networks. To have an idea of the importance of non linear effects in those relationships it should be recalled that the values of the angle of incidence ψ in Figure 10, due to the fluctuating components of wind velocity can vary between ± 10, as shown in Figure 11, (full scale measurements on the Humber bridge, Bocciolone et al. 1990). Being well known that the flutter derivatives are highly sensitive to the average angle of attack (Zasso 1993a), as a consequence, because of those non linearities, the aerodynamic forces due to turbulence and to deck motion can not be calculated separately and then superposed. Nevertheless, several methods are still based on the separation of the aerodynamic forces due to turbulence from those due to bridge motion, as in (Bucher 1992a,b). Bucher's method adopts the quasi-static corrected theory for modelling the aerodynamic forces related to turbulence. The forces depending on the deck's motion are calculated by means of the convolution integral, with deck's displacements and rotation (and their derivatives) as inputs. To this end, the wind forces

response to an impulsive variation of each single input (defined as a superposition of exponential functions), is obtained through an identification procedure performed on the results of wind tunnel measurements similar to those adopted for the extraction of the flutter derivatives. As far as the contribution due to deck's motion is concerned, and assuming the problem as linear, this solution of the problem is rigorous, reproducing the unsteady aerodynamic forces. This method could be further improved, as proposed in (Li 1997) introducing indicial functions also for that portion of forces due to wind turbulence. In fact, the use of indicial functions in time domain corresponds to the use of admittance functions in the frequency domain, but an additional advantage is represented by the possibility of suitably taking into account the effects of bridge motion transients and time variation of incident flow. Nevertheless, the non-linearities cannot be taken into account by this approach. Moreover, the transformation from flutter derivatives to indicial functions is not straightforward and therefore the identification of the parameters of these indicial functions could be problematic. This topic is not highlighted in the mentioned references. Another approach (Miyata 1995) adopts a quasi-steady formulation of the wind forces, considering the instantaneous angle of attack between the incident flow and the deck (ψ in Figure 10) and using the section model static aerodynamic coefficients measured in wind tunnel. The quasi-static formulation is as follows:

$$\begin{aligned} F_L &= \tfrac{1}{2}\rho b V^2 C_L(\alpha) & F_z &= F_L\cos\psi + F_D\sin\psi \\ F_D &= \tfrac{1}{2}\rho b V^2 C_D(\alpha) & F_y &= -F_L\sin\psi + F_D\cos\psi \\ M &= \tfrac{1}{2}\rho b^2 V^2 C_M(\alpha) & & \\ \alpha &= \vartheta - \psi & V^2 &= \left(W - \dot{z} + b_1\dot{\vartheta}\right)^2 + \left(U - \dot{y}\right)^2 \end{aligned} \qquad (1)$$

where F_z, F_y and M are respectively the vertical force, lateral force and moment per deck unit length, C_D,C_L and C_M are the static lift, drag and moment coefficients of the deck, measured as functions of the angle of attack α. Defining the vector $\{q\}$ as follows, equations (1) become:

$$\underline{q}^T = \{y \;\; z \;\; \vartheta \;\; U \;\; W\} \qquad F^T = \{F_y \;\; F_z \;\; M_x\} \qquad \underline{F} = \underline{F}\{q, \dot{q}\} \qquad (2)$$

With this theory, deck motion, wind turbulence effects and static effects are all included at the same time and the dependence of the aerodynamic forces on the actual angle of attack, is considered. On the other hand, this approach does not take into account the dependence of the aerodynamic coefficients on the reduced velocity $V^*=U/(fB)$ and therefore its applications should be in principle limited to those cases where V^* is sufficiently high (corresponding in other words to the situations where the time taken by the flow to cross the section is much shorter than the oscillation period of the structure or than the period associated with the incoming turbulence fluctuations, approaching the steady-state conditions). The aerodynamic forces acting along the deck can be calculated according to (2) and then reduced to the degrees of freedom of the structure, generally the nodal co-ordinates of a finite element schematisation, while in some cases modal reduction is also used. The non-linear motion equations have therefore the general form:

$$[M_s]\,\ddot{\underline{X}} + [R_s]\,\dot{\underline{X}} + [K_s]\,\underline{X} = \underline{F}_a(\underline{X}, \dot{\underline{X}}, t) \qquad (3)$$

being $[M_s]$, $[R_s]$ and $[K_s]$ the structural matrices of the bridge, and $\underline{F}_a$ the vector of the generalised forces due to wind action, function of the bridge motion and of the space-time history of turbulent wind. In (Miyata et al. 1995), comparisons with the results of the 1:100 aeroelastic model of Akashi bridge are also reported. Expressions (1) are effective, as already said, for reduced velocities $V^*=V/\omega B$ sufficiently greater than 10. If V^* is smaller, these expressions fail and the dependence of these expressions from the reduced velocity must be introduced or another theory must be developed. In order to reach this goal, the "quasi-static corrected theory" was developed (Diana 1993b, Diana 1994). For a better understanding, the equations (2) are linearised around a reference angle of attack α_0 defined both by the value of the horizontal U_0 and vertical W_0 component of the wind, and by the motion of the section itself defined by the

following values y_o, $\dot{y}_o$, z_o, $\dot{z}_o$, ϑ_o, $\dot{\vartheta}_o$. In other words, with reference to equation (2), $\underline{F}\{q, \dot{q}\}$ is linearised around $\{q_o, \dot{q}_o\}$ values giving:

$$\underline{F} = \underline{F}_0 + \left[\frac{\partial \underline{F}}{\partial \underline{q}}\right]_0 \underline{\Delta q} + \left[\frac{\partial \underline{F}}{\partial \underline{\dot{q}}}\right]_0 \underline{\Delta \dot{q}} = \underline{F}_0 + \left[K_{F0}\right] \underline{\Delta q} + \left[R_{F0}\right] \underline{\Delta \dot{q}} \tag{4}$$

$$[K_{F0}] = \frac{1}{2}\rho b V_0 \begin{bmatrix} 0 & 0 & g_3(K_{D0}\cos\alpha_0 - K_{L0}\sin\alpha_0)V_0 & 2(C_{D0}\cos_0 - C_{L0}\sin\alpha_0) & ((K_{L0} - C_{D0})\sin\alpha_0 - (K_{D0} + C_{L0})\cos\alpha_0) \\ 0 & 0 & h_3(K_{D0}\sin\alpha_0 + K_L\cos\alpha_0)V_0 & 2(C_{D0}\sin_0 + C_{L0}\cos\alpha_0) & -(K_{L0} - C_{D0})\cos\alpha_0 - (K_{D0} + C_{L0})\sin\alpha_0 \\ 0 & 0 & a_3 K_{M0} b V_0 & 2bC_{M0} & -bK_M \end{bmatrix} \tag{5}$$

$$[R_{F0}] = \frac{1}{2}\rho b V_0 \begin{bmatrix} -2g_4(C_{D0}\cos\psi_0 - C_{L0}\sin\psi_0) & -g_i((K_{L0} - C_{D0})\sin\psi_0 - (K_{D0} + C_{L0})\cos\psi_0) & g_2 b_{1y}((K_{L0} - C_{D0})\sin\psi_0 - (K_{D0} + C_{L0})\cos\psi_0) & 0 & 0 \\ -2h_4(C_{D0}\sin\psi_0 + C_{L0}\cos\psi_0) & -h_1(-(K_{L0} - C_{D0})\cos\psi_0 - (K_{D0} + C_{L0})\sin\psi_0) & h_2 b_{1z}(-(K_{L0} - C_{D0})\cos\psi_0 - (K_{D0} + C_{L0})\sin\psi_0) & 0 & 0 \\ -2a_4 C_{M0} b & a_1 K_{M0} b & -a_2 b_1 K_{M0} b & 0 & 0 \end{bmatrix} \tag{6}$$

being:

$$\begin{array}{llll} \alpha_o : \text{reference angle} & K_{D0} = \left(\frac{\partial C_D}{\partial \alpha}\right)_{\alpha=\alpha_0} & K_{L0} = \left(\frac{\partial C_L}{\partial \alpha}\right)_{\alpha=\alpha_0} & K_{M0} = \left(\frac{\partial C_M}{\partial \alpha}\right)_{\alpha=\alpha_0} \\ V_o^2 = \sqrt{U_o^2 + W_o^2} & C_{D0} = C_D(\alpha)_{\alpha=\alpha_0} & C_{L0} = C_L(\alpha)_{\alpha=\alpha_0} & C_{M0} = C_M(\alpha)_{\alpha=\alpha_0} \end{array} \tag{7}$$

The coefficients $h_i = h_i(V^*, \alpha_o)$, $g_i = g_i(V^*, \alpha_o)$ and $a_i = a_i(V^*, \alpha_o)$ (i = 1, 4), corresponding to the "flutter derivatives" measured on section models (Scanlan 1971, Singh 1995, Zasso 1996), have been introduced in the aerodynamic forces equivalent stiffness and damping matrices in order to represent their dependence on the reduced velocity V^*. If the appropriate b_{1z}, b_{1y} and $b_{1\theta}$ values are introduced (the ones holding in quasi-static conditions), the consistency with a quasi-static approach is shown by the convergence to unity of h_i, a_i and g_i increasing V^*. No corrective coefficients were introduced for turbulence dependent terms. These expressions become similar to the Scanlan flutter derivatives formulation (Scanlan 1971) if no turbulence and no horizontal deck motion are considered and if a linearisation is done around zero motion of the deck. In this case matrices (6) and (7) become:

$$\left[\hat{K}_{Fo}\right] = \frac{1}{2}\rho b V_0^2 \begin{bmatrix} 0 & 0 & 0 & 0 & 0 \\ 0 & 0 & h_3 K_L & 0 & 0 \\ 0 & 0 & a_3 K_M b & 0 & 0 \end{bmatrix} \quad \left[\hat{R}_{Fo}\right] = \frac{1}{2}\rho b V_0 \begin{bmatrix} 0 & 0 & 0 & 0 & 0 \\ 0 & h_1(K_{L0} - C_{D0}) & -h_2 b_{1z}(K_{L0} - C_{D0}) & 0 & 0 \\ 0 & a_1 K_{M0} b & -a_2 b_1 K_{M0} b & 0 & 0 \end{bmatrix} \tag{8}$$

Figure 12 shows, for the final Messina Bridge deck solution, two of the a_i^* and h_i^* corrective coefficients of the "quasi-static theory" normalised assuming b_{1z}, b_{1y} and $b_{1\theta}$ equal to the chord b and constant C_{D0}, K_{L0} and K_{M0} values for the different angles of attack (for a full reference see Zasso 1993a). The diagrams confirm that the "quasi-static theory" is effective with high V^* reduced velocities as the zero angle of attack coefficients go to unity for $V^* > 10$.
These linear expressions of aerodynamic forces will be used in the following discussion of the corrected quasi-static theory method: they are similar to those of Scanlan and the advantages are related only to a better physical understanding. The method consists in dividing the wind spectrum, as shown in Figure 13, into a low frequency range, labelled "0", and in many high frequency sub-ranges, labelled "1", "2", etc. The upper values of the "0" frequency range is defined by the lower value of the reduced velocity for which the quasi-static assumption is still valid, for example $V^*=10$. For each of these contributions, a separate space-time history can be generated: in the following U_0, W_0 represent the time histories of the horizontal and vertical components of the low frequency contribution ("0" range including the mean value), while ΔU_1, ΔW_1, ΔU_2, ΔW_2, ... represent the different high frequency contributions. It should be remarked that the hypothesis of the quasi-steady theory apply only to the "0" contributions.

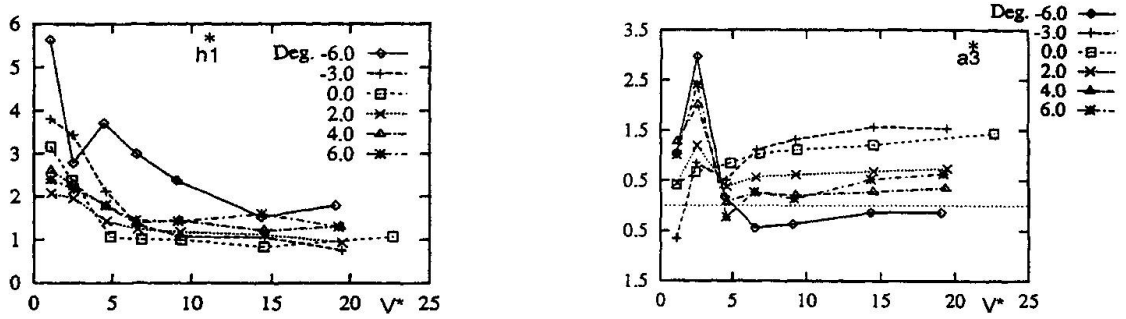

Figure 12 Final Messina Bridge deck design: "corrected quasi-static theory" a_3^* and h_1^* coefficients versus reduced V^* wind velocity as a function of the mean α_o angle of attack [Deg]. The values here reported refer to the assumption of b_{1z}, b_{1y} and $b_{1\theta}$ equal to b.

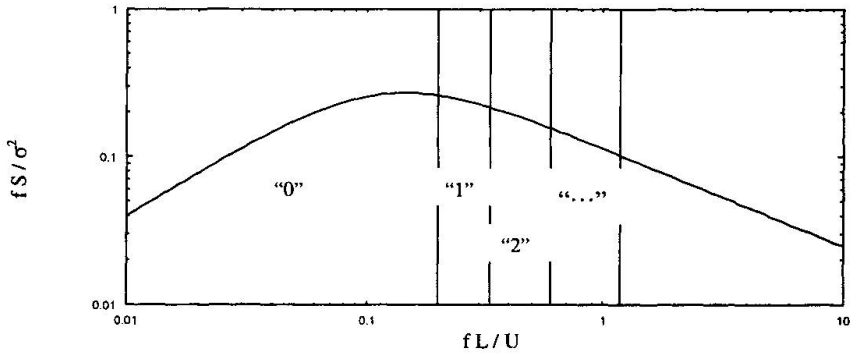

Figure 13 Normalised wind spectrum divided in frequency sub-ranges

In the same way, the total response of the bridge $\underline{X}(t)$ is considered as the superposition of different contributions $\underline{X}_0$, $\underline{X}_1$, ... , corresponding to the frequency ranges previously introduced for the wind turbulence:

$$\underline{X}(t) = \underline{X}_0(t) + \underline{X}_1(t) + \underline{X}_2(t) + \ldots \tag{9}$$

As a first step, disregarding the effects of high frequency wind and motion terms, the low frequency response $\underline{X}_0(t)$ of the structure can be calculated according to the quasi-static theory, by means of the following set of motion equations:

$$[M_s]\ddot{\underline{X}}_0 + [R_s]\dot{\underline{X}}_0 + [K_s]\underline{X}_0 = \underline{F}_a(\underline{X}_0, \dot{\underline{X}}_0, t) \quad [1] \tag{10}$$

In this way the non-linear dependence of the aerodynamic forces on the angle of attack is kept into account and, on the other side, the use of the quasi-steady theory is justified by the fact that in the considered range of frequencies the aerodynamic coefficients are reduced velocity-independent. For what concerns the high frequency contributions to the bridge motion, the motion equations are linearised around the low frequency component $\underline{X}_0(t)$ previously defined. Expressions (5) and (6) represent the linearised aerodynamic forces applied in a generic deck section, and being $\underline{X}_0$ a dynamic solution, the expressions become linear but with time dependent coefficients. This represents a reasonable approximation since the main variations of the angle of attack are related to the range of low frequencies. In other words, components ΔU_1, ΔW_1, are considered small with respect to U_0, W_0 and correspondingly, the $\underline{X}_1$, $\underline{X}_2$, ... components of motion are assumed small with respect to $\underline{X}_0$. In order to take advantage of the knowledge of $h_i=h_i(V^*,\alpha_o)$, $g_i=g_i(V^*,\alpha_o)$ and $a_i=a_i(V^*,\alpha_o)$, functions of the wind reduced velocity and of α_o, a

[1] The integration of this non linear equation is done numerically, filtering the frequencies that are over the "0" frequency range.

modal approach is introduced for each sub-range, considering only the modes pertaining to that particular range of frequency:

$$\underline{X}_1 = [\Phi_1]\underline{q}_1 \quad ; \quad \underline{X}_2 = [\Phi_2]\underline{q}_2 \quad ; \quad \ldots \tag{11}$$

where $[\Phi_1]$ represents the modal shapes matrix corresponding to the bridge natural frequencies falling in the "1" frequency range, $\underline{q}_1$ is the corresponding vector of modal co-ordinates and so on. A separate set of equations of motion is then written for each sub-range, neglecting the coupling terms between the different sub-ranges. In each of these sets of equations, the appropriate value of corrective coefficients is used, according to the value of the reduced velocity pertaining to the sub-range. It must be again pointed out that, since the equations of motion are linearised around the $\underline{X}_o$ solution, the flutter derivatives are modulated by the variation of the angle of attack corresponding to $\underline{X}_o$ solution, so that the equations are linear, but with time dependent coefficients. The results of this method have been compared with both full-scale measurements (Humber bridge, Diana 1990, Diana 1994) and with wind tunnel tests on a 1:250 scale full bridge aeroelastic model (Messina Bridge, Diana 1995). A detailed illustration of the experimental results compared to the numerical simulations of those test cases can be found also in (Diana 1998). Figure 14 shows a photograph of the Messina Bridge aeroelastic model in the Danish Maritime Institute (D.M.I.) wind tunnel in Copenhagen.

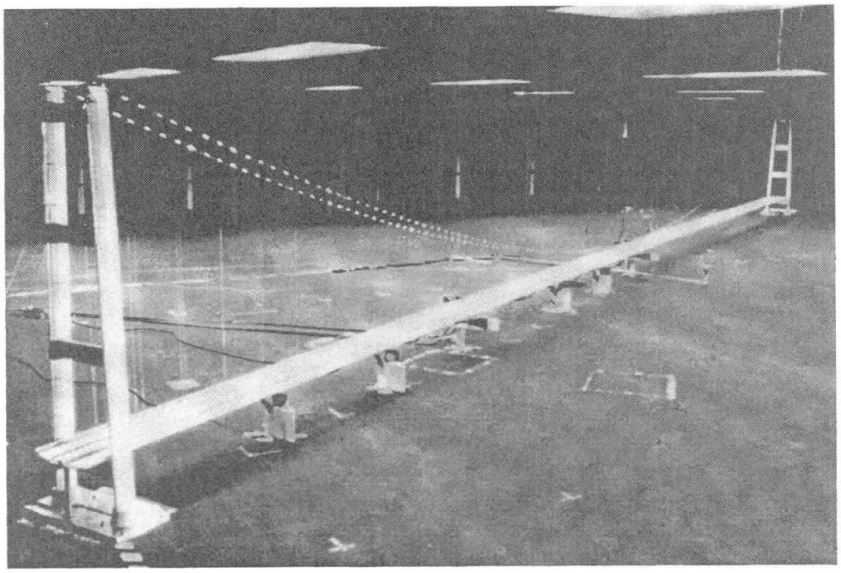

Figure 14 The Messina Bridge full model in the D.M.I. tunnel

The analysis and comparison of the numerical and experimental wind tunnel results was very interesting, showing substantial good agreement. The consistency of the experimental and numerical results in the over mentioned test cases gave confidence for the extension of the numerical simulation approach to the real Messina Bridge behaviour. As an example, Figure 15 shows the trend of the first torsional frequency of the bridge and the related damping factor as a function of the wind speed: these results are obtained both using the 3D full model in the experimental wind tunnel tests and using the numerical simulation model. As it can be observed, a good correspondence between the numerical and the experimental results is obtained. The not negligible difference in the experimental values of damping factor obtained in smooth-flow and turbulent-flow conditions is anyway something that needs further investigations. It can be underlined the importance of these kind of analysis as they allow to obtain some meaningful parameters for the stability definition.
The knowledge of the stability index ($h = r/r_c$), as a function of the mean wind speed, allows both to evaluate with precision the instability threshold (defined as the wind velocity corresponding to zero value of the non-dimensional damping factor) and also to define the stability index value at the design maximum velocity (62 m/s for the Messina bridge). In the Messina Bridge case, the instability index value at the design wind speed is 4% for the first torsional mode (see Figure 15), being the non-dimensional structural damping factor $\cong$1%. This result means that the aero-

elastic deck design adds to the bridge an high aerodynamic damping, at the maximum design wind speed. A high value of the instability index means also a low buffeting response of the bridge to the turbulent wind as it was confirmed from the measured response of the full model in wind tunnel tests and from the numerical simulation.

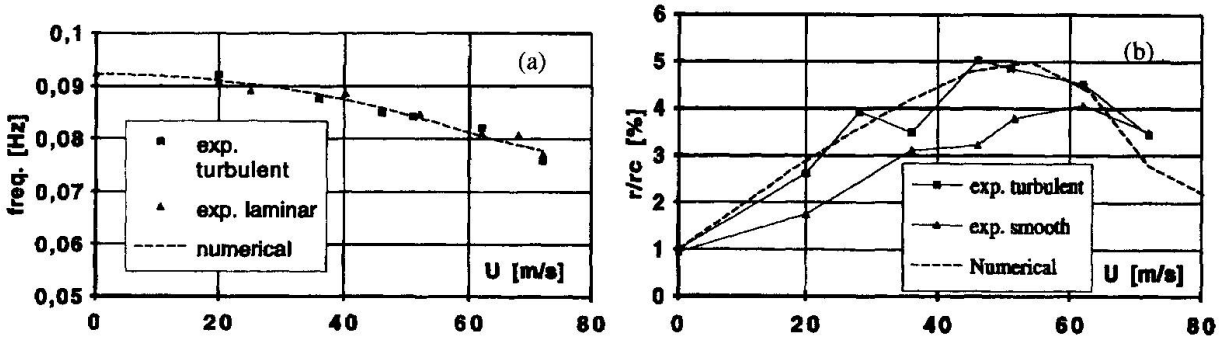

Figure 15 Messina bridge: comparison between numerical and experimental wind tunnel full model results: first torsional mode: (a) frequency and (b) damping factor variation as a function of the wind speed (real scale)

5 Concluding Remarks

The following conclusions can be drawn:

- Some possible strategies for the design of suspension bridges with span length greater than 3000m are available, and some of them have been proved to be feasible.
- The accurate simulation of the bridge response to turbulent wind, and the estimate of the corresponding instability indexes, are fundamental tools for the assessment of the bridge feasibility and for its final check.
- On the other hand, simplified methods, which do not take into account all the aspects of the aeroelastic problem, if applied to non conventional solutions, may result highly inaccurate for the selection of an optimal solution. Particular care is required in the separation of the static problem from the dynamic one, or in the modal approach applied to non conventional typologies, where limiting the analysis of the critical speed to only a couple of modes could be misleading.
- The development of the field of wind engineering, with particular reference to wind-bridge interactions, requires a validated procedure for the calculation of the bridge response to turbulent wind: this could be done by means of a benchmark test on the existing simulation codes.

References

Achkire Y., Preumont A., 1997. Flutter control of cable-stayed bridges, *2nd EACWE Int. Conf., Genova, Italy*

Astiz M.A., 1993. Wind resistant design of the Gibraltar Strait crossing bridge, *International Seminar on Utilization of Large Boundary Layer Wind Tunnel, Tsukuba, Japan*

Astiz M.A., 1996. Wind related behaviour of Alternative Suspension Systems, *15 th IABSE, Copenhagen, Denmark*

Bocciolone M., Cheli F., Curami A., Zasso A. 1990. Wind measurements on the Humber bridge and numerical simulations. *Proc. 8th Int. Conf. On Wind Eng. ICWE, London, Ont., Canada*

Borri. C., Majowiecki M., Spinelli P., 1992. Sul vantaggioso comportamento, sotto l'azione del veto, di un ponte di grande luce in tensostruttura a doppio effetto, *2° Nat. Conf. Wind Eng. IN-VENTO-92, Capri, Italy*

Brown W., 1996. Development of the deck for the 3300m span Messina crossing, *15th IABSE, Copenhagen*

Bucher G. C., Wall F. J.,1992a. Probabilistic description of buffeting response of long span bridges. Part I: basic concepts. *J. Of Engineering Mechanics ASCE* Vol. 118 n.12 pp. 2401-2420

Bucher G. C., Wall F. J.,1992b. Probabilistic description of buffeting response of long span bridges. Part II: extended analysis. *J. Of Engineering Mechanics ASCE* Vol. 118 n.12 pp. 2421-2441

Cobo del Arco D., Aparicio Bengoechea A.C., 1997. Some proposals to improve the wind stability performance of long span bridges, *2nd EACWE International Conference, Genova, Italy*

Diana G., Cheli F., Collina A., Zasso A., Brownjohn J., 1990. Suspension bridge parameter identification in full scale tests. *In Proc. 8th Int. Conf. On Wind Engineering, London, Ont., Canada*

Diana G., 1993a. Analytical and wind-tunnel simulations for the aeroelastic design of the Messina Straits Bridge, *International Seminar on Utilization of Large Boundary Layer Wind Tunnel, Tsukuba, Japan*

Diana G., Bruni S., Cigada A., Collina A. 1993b. Turbulence effects on flutter velocity in long span suspended bridges, *J. of Wind Eng. and Ind. Aer.* 48 pp. 329-342

Diana G. et al., 1994. On the response of a long span bridge to turbulent wind: comparison between numerical simulation and experimental results, *3rd Italian Nat. Cong. of Wind Eng. IN-VENTO-94, Rome, Italy (in italian)*

Diana G., et al., 1995. Comparisons between wind tunnel tests on a full aeroelastic model for the proposed bridge over Stretto di Messina and numerical results, *J. of Wind Eng. and Ind. Aer.* 54/55 pp. 101-113

Diana G., et al., 1998. Experience gained in the Messina Bridge aeroelastic project, *International Seminar on Long Span Bridge Aerodynamics Perspective '98, Kobe, Japan.*

Dyrbye C., Hansen S. O., 1997. Wind loads on structures, *John Wiley & Sons*

Gimsing N. J., 1994. Suspended bridges with very long spans, *International Conference AIPC - FIP on Cable-Stayed and Suspension Bridges, Deauville, France*

Gimsing N. J., 1997. Cable supported bridges, John Wiley & Sons, 1997

Ito M., 1996. Super long span cable-suspended bridges in Japan, *15 th Congress IABSE Copenhagen, Denmark*

Larose G.L. et al.,1997, Direct measurements of buffeting wind forces on bridge decks, *2nd EACWE, Genova, Italy*

Leonhardt F., 1968. Die Entwicklung aerodynamisch stabiler Hangebrucken, *Die Bautechbik, Hefte 10 und 11*

Li M., Dexin H. 1997. Aerodynamic admittance of bridge deck sections, *2nd EACWE Int. Conf., Genova, Italy*

Meier U., 1991. Modern materials in bridge engineering, *IABSE Symposium, pp. 311-323, Leningrad*

Miyata T., Sato H., Kitagawa M., 1993. Design considerations for superstructures of the Akashi Kaikio bridge, *International Seminar on Utilization of Large Boundary Layer Wind Tunnel, Tsukuba, Japan*

Miyata T., Yamada H., Boonyapinyo V., Santos J. C., 1995. Analytical investigation on the response of a very long suspension bridge under gusty wind, *Proc. 9th Int. Conf. On Wind Engineering, ICWE, New Delhi, India*

Miyata T., Yamada H., Dung N. N., 1996. Proposed measures for flutter control in long span bridges, *15 th Congress IABSE, Copenhagen, Denmark*

Miyazaki M., Arai M., Kazama K., Kubota H., 1997. Stay-cable systems of long span suspension bridges for coupled flutter, *2nd EACWE International Conference, Genova, Italy*

Musmeci S., 1971. La campata di 3000 m di Musmeci, *L'Industria delle Costruzioni, n° 22, pp. 10-27*

Nomura K., Nakazaki S. et al., 1994. Comparison of different cable systems on the static and coupled flutter characteristics of a 3000 m class suspension bridge, *Int. Conf. AIPC - FIP on Cable-Stayed and Suspension Bridges, Deauville, France*

Ogawa K., Shimodoi H., Nogami C., 1997. Aerodynamic Stability of super-long span suspension bridge with 2-box and 1-box combined girder, *2nd EACWE International Conference, Genova, Italy*

Ostenfeld K. H., Larsen A., 1992. Bridge engineering and aerodynamics, *Aerodynamics of Large Bridges, Proc. First Int. Symp. on Aerodyn. of Large Bridges, Copenhagen, Denmark*

Reinhold T., Larsen A., Damsgaard A., Svensson E., 1993. The role of full bridge model tests in wind engineering studies for the Great Belt east suspension bridge, tunnel, *Int. Sem. on utilization of large boundary layer wind tunnels, Tsukuba, Japan*

Scanlan R.H., Tomko J.J., 1971, Airfoil and bridge deck flutter derivatives, *ASCE J. Eng. Mech. Div., 97, No.EM6*

Scanlan R. H., 1992, Wind dynamics of long-span brdiges, *Aerodynamics of Large Bridges, A. Larsen Ed., Balkema, Rotterdam*

Singh, L., Jones N.P., Scanlan R.H., Lorendeaux O., 1995, Simultaneous Identification of 3-DOF Aeroelastic Parameters *9th International Conference on Wind, New Delhi, India, 9-13 January 1995*

Shinozuka M., Jan C.M., 1972, Digital simulation of random processes and its applications, *Journal of Sound and Vibration, 25(1, 111-128)*

Sumiyoshi Y., Endo T., Miyata T., Sato H., Kitagawa M., 1993. Experiments for the Akashi-Kaikyo in a large boundary layer wind tunnel, *Int. Sem. on utilization of large boundary layer wind tunnels, Tsukuba, Japan*

Walther R., Amsler D., 1994. Hybrid suspension systems for very long span bridges: aerodynamic analysis and cost estimates, *International Conference AIPC-FIP on Cable-Stayed and Suspension Bridges, Deauville, France*

Zasso A., Curami A., 1993a. Extensive Identification of Bridge Deck Aeroelastic Coefficients: Average Angle of Attack, Reynolds Number and Other Parameter effects, *3rd Asian-Pacific Symp. on Wind Eng., Hong Kong*

Zasso A, Cigada A., Curami A., Paini A., 1993b. Ponte sospeso per l'attraversamento dello Stretto di Messina: ottimizzazione aerodinamica e aeroelastica dell'impalcato su modello sezionale in scala 1:30, *Rapporto Interno del Dipartimento di Meccanica del Politecnico di Milano 05-93*

A. Zasso, 1996. Flutter Derivatives: Advantages of a New Representation Convention, *J.W.E.I.A. 60 (1996) 35-47*